

Crosstalk Measurements in the Electromagnetic Calorimeter during ATLAS Final Installation

Renat Ishmukhametov*, Julien Labbé†

Abstract

Various types of crosstalk measured with calibration runs at ATLAS final installation stage, both in the barrel and the endcap electromagnetic calorimeters, are reviewed and compared with previous beam tests results. This note also shows how crosstalk analysis is a good tool to characterize misbehaving channels and gives the taxonomy of the main observed pathologies.

1 Introduction

A feature that affects energy reconstruction in the ATLAS electromagnetic calorimeter is signal leakage from a cell recording a physical or calibration signal to other cells, which is called crosstalk. The leakage can originate on the electrodes or come through the electronic chain, leading to three types of crosstalk: capacitive, resistive and inductive. A detailed study of the different sources of crosstalk can be found in the reference [1].

Measurements and studies of the crosstalk have been done during the test beam analysis in 1999-2001 for the barrel [2][3] and for the endcap [5] calorimeters. The aim of the current work is to give a summary of crosstalk measurement from the recent calibration runs taken during the final detector installation.

A detailed description of the calorimeter's calibration schemes is presented in reference [6]. The method used for calibration consists of sending a pulse that mimics the physical signal to a calorimeter channel and testing the response of the readout chain. The generated signal is produced by the calibration boards located outside of the cryostat in the electronics crate that houses the readout front-end boards. The signal is sent to

*Department of Physics, Southern Methodist University, Dallas, TX 75275, USA.

†Laboratoire de Physique Subatomique et Cosmologie, Université Joseph Fourier Grenoble 1, CNRS/IN2P3, Institut Polytechnique de Grenoble, Grenoble, France.

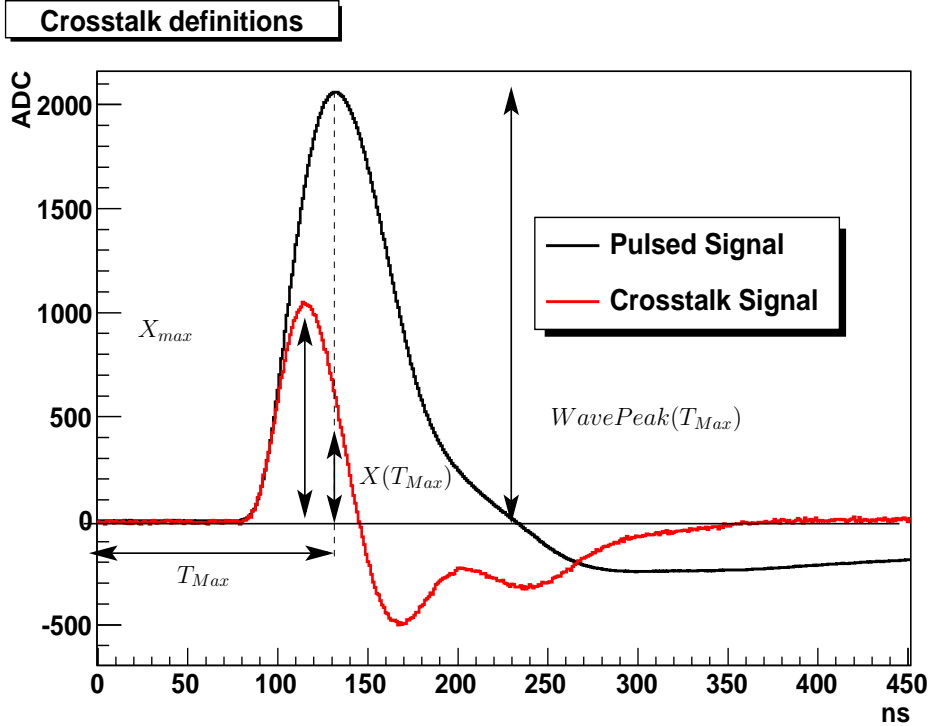


Figure 1: Two different crosstalk definitions. Peak-peak crosstalk is defined as $X_{max}/WavePeak(T_{max})$ where X_{max} is the crosstalk amplitude. Under-peak crosstalk is defined as $X(T_{max})/WavePeak(T_{max})$ where $X(T_{max})$ is the crosstalk signal value at the time T_{max} .

the motherboard, which is located in the liquid argon calorimeter cryostat close to the accordion electrodes.

In Figure 1 is shown an example of a signal in a pulsed channel and a signal in the channel next to the pulsed one together with the parameters used in the crosstalk definition. There are two ways to define the crosstalk value [1], [3]. The first way is to use the ratio of the crosstalk signal peak value to the peak value of the pulsed signal. This will be referred to as peak-peak crosstalk. Another way is to calculate the ratio of the crosstalk signal to the pulsed signal at the pulsed channel peak time. This definition will be referenced as under-peak crosstalk.

The most important effect of the crosstalk is that it modifies the position and the value of the pulsed channel peak. This affects the energy calculation and the calibration constant computation by biasing the arguments of the ramp coefficients, characterizing the readout chain linearity [6]. The more the crosstalk changes the wave amplitude, the more it affects the energy reconstruction. The under-peak definition is closely related to the change of the amplitude of the pulsed signal and thus is more relevant. However, it is very sensitive to the exact shape of the crosstalk signal and thus subject to large

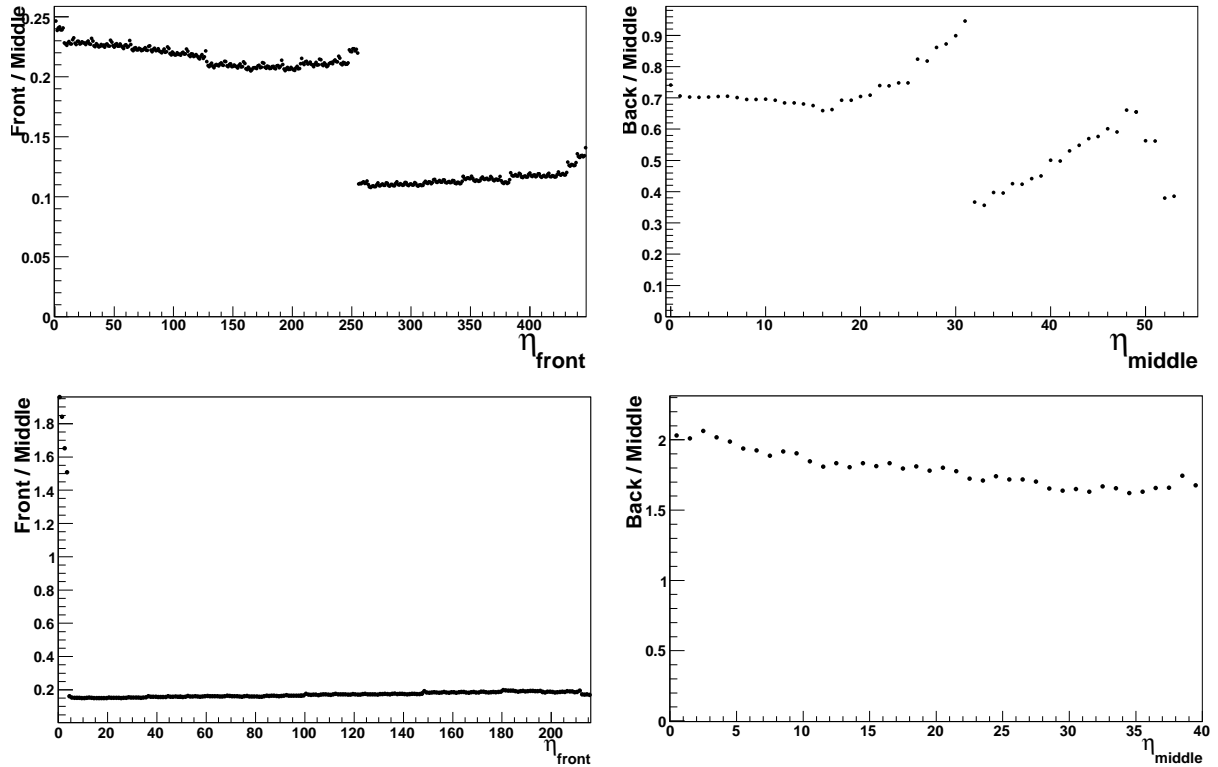


Figure 2: Ratio of gain factors (MeV/ADC), in the barrel (top) and the endcap (bottom), between the front (left) or back (right) sampling cells and the middle ones as function of the cells numbering along η .

fluctuations. The peak-peak definition provides an overestimated crosstalk value at the peak but allows a clearer understanding of the crosstalk effect. It can be used as an upper limit of the crosstalk. At this point, only the crosstalk in the front sampling is corrected in the Optimal Filtering Coefficients¹ and ramp computation[9].

The calibration scheme is designed in such a way that even though many channels are pulsed at the same time, neighbouring channels are not pulsed simultaneously (see annex A), allowing the study of the crosstalk in the neighbourhood of the pulsed channel, where the crosstalk is higher. Our results are in general normalised to the case where only one channel is pulsed: the calibration scheme and channel layout are taken into account when necessary by correction factors explained in annex A.

To deal with physical quantities, gain factors converting ADC counts to energy measurement have been applied to the measured amplitudes. The effects of these gain factors are relevant mainly to the study of the crosstalk between the different layers of the calorimeter: the ratio between the gain factors in the different samplings is presented in

¹See [6] for the definition of the Optimal Filtering Coefficients.

Figure 2. All crosstalk results in this note refer to energy after application of these factors. In this figure, and for all the others, the two sides of the calorimeter have been averaged, and channels are numbered in each sampling with growing η values in the barrel or the endcap.

The main sources of crosstalk between all cells in the detector have been identified and quantified. In the front sampling the crosstalk mainly originates from capacitive coupling on the electrodes and reaches its highest values. Its study is presented in section 2. The crosstalk between the middle and front layers comes principally from the ink resistors on the high voltage (HV) electrodes. It is discussed in section 3. In and between the middle and back samplings the crosstalk is dominated by inductive couplings. This crosstalk is detailed in section 4. Finally, section 5 details the information provided by crosstalk analysis relevant to characterizing misbehaving channels.

2 Capacitive Crosstalk in the Front Sampling

2.1 Origin

The capacitive coupling originates between the electrodes themselves. It is the main source of crosstalk in the front sampling where the segmentation is high. In the middle and back samplings the capacitive coupling is dominated by the inductive one (see section 4). This section focuses on short distance crosstalk between the front layer cells, or strips, namely: strip to neighbour strip and strip to next to neighbour strip crosstalk.

The scheme of the capacitive coupling in the electrode is shown in Figure 3. During calibration or after liquid argon ionisation the injected current I_d is shared between the pulsed cell and its neighbour with the respective currents I_s and I_X . Cells are read through the preamplifier input impedances R_{in} . The capacitive crosstalk is proportional to the ratio C_d/C_x [1], where C_d and C_x are the detector and crosstalk capacitance respectively. This crosstalk affects the η neighbours of the channels.

The typical shapes of a signal in the η neighbour and next to neighbour of a pulsed cell are shown in Figure 4. The shape of the first neighbour is close to the derivative of the waveform of a pulsed signal, as expected for capacitive coupling [1]. The signal in the next to neighbour is more distorted, but remains close to the second derivative of the initial pulse.

2.2 Crosstalk measurements

Average crosstalk values in the front sampling for 2008 data in the neighbour and next to neighbour of a pulsed strip are summarized and compared with the previous test beam 2001-2002 and 1999 measurements in Table 1. The agreement is very satisfactory: the

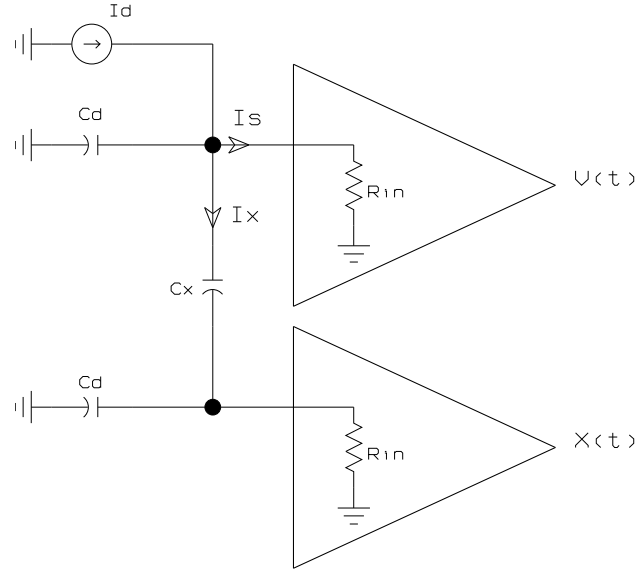


Figure 3: Schematic of the capacitive crosstalk between two neighbour channels (from [1]).

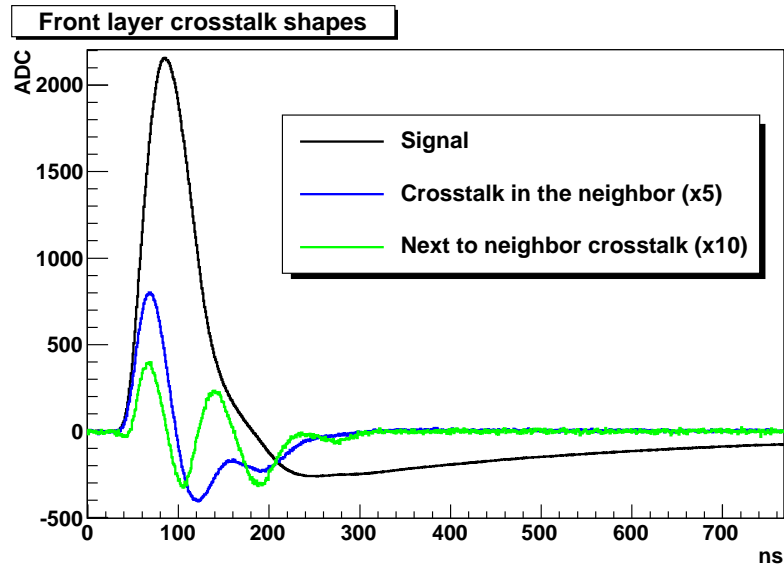


Figure 4: Typical shapes of the crosstalk signals in the front layer. The neighbour in η channel shape is scaled by factor 5, the next to neighbour in η by factor 10.

whole detector crosstalk in the front sampling behaves as expected based on previous studies of test modules.

It should be noticed that the crosstalk is uniform along Φ . In Figure 5 it is shown

Crosstalk type	Barrel		Endcap	
	peak-peak	under-peak	peak-peak	under-peak
Strip to neighbour strip	7.16 %	4.34 %	6.33 %	3.8 %
RMS	0.90 %	0.60 %	1.1 %	0.67 %
Test beam measurements	7.26 %	4.3 %	6.4 %	3.7 %
Strip to next to neighbour strip	0.78 %	0.22 %	0.89 %	0.40 %
RMS	0.17 %	0.12 %	0.10 %	0.12 %
Test beam measurements	0.88 %	0.3 %	< 0.5 %	< 0.5 %

Table 1: Strip layer crosstalk present (2008) results compared with the previous (1999 and 2001-2002 test beam) data [2] [5].

the distribution of the relative dispersion along Φ (that is the ratio for of the RMS to the mean for each set of channels with the same value of η). The relative dispersion is less than 10 %, except the under-peak next to neighbour crosstalk where the value ~ 35 % comes from the fast variation of the crosstalk signal under the peak of the pulsed channel.

The other part of this section is focused on the dependence of the crosstalk value with η .

2.2.1 Strip to neighbour strip crosstalk

The strip to neighbour strip peak-peak crosstalk ranges between 6 and 9 % in the barrel (between 4 and 5 % for under-peak crosstalk) and between 4 and 8 % in the endcap (resp. 2 and 5 %). The η dependency for both crosstalk definitions is shown in Figures 6 and 7.

A systematic dip can be found every 8/12/8 channels in the endcap and every 16/8 channels in the barrel. This can be explained by a capacitive coupling in the summing board connectors on the motherboards. This gives an additional crosstalk of ~ 2 % with the peak-peak definition and ~ 1 % with under the peak definition, which disappears for the channels at each edge of the connector. The repartition of the dips varies with the different cablings on the motherboards. In the barrel the cabling is different for electrodes A ($\eta_{front} \leq 256$, 16 channels per connector) and B ($\eta_{front} > 256$, 8 channels per connector) [3]. The very low value at $\eta_{front} = 255$ is due to the change of electrodes.

In the endcap, the cabling varies with regions. Region 2 ($4 \leq \eta_{front} \leq 99$) has 8 channels per motherboard connector, region 3 ($100 \leq \eta_{front} \leq 147$) has 12 channels per motherboard connector, and region 4 ($148 \leq \eta_{front} \leq 211$) has 8 channels per motherboard connector.

The size of cells in the endcap also varies with regions. Regions 2, 3 and 4 have 8, 6 and 4 cells per 0.025 units in η respectively. The change of granularity provides the overall decrease of the crosstalk value as a function of η . The first four and the last four cells of the front layer ($0 \leq \eta \leq 3$ and $212 \leq \eta \leq 215$) are much larger than the other cells. Thus the capacitive coupling is dominated in this region by the inductive coupling.

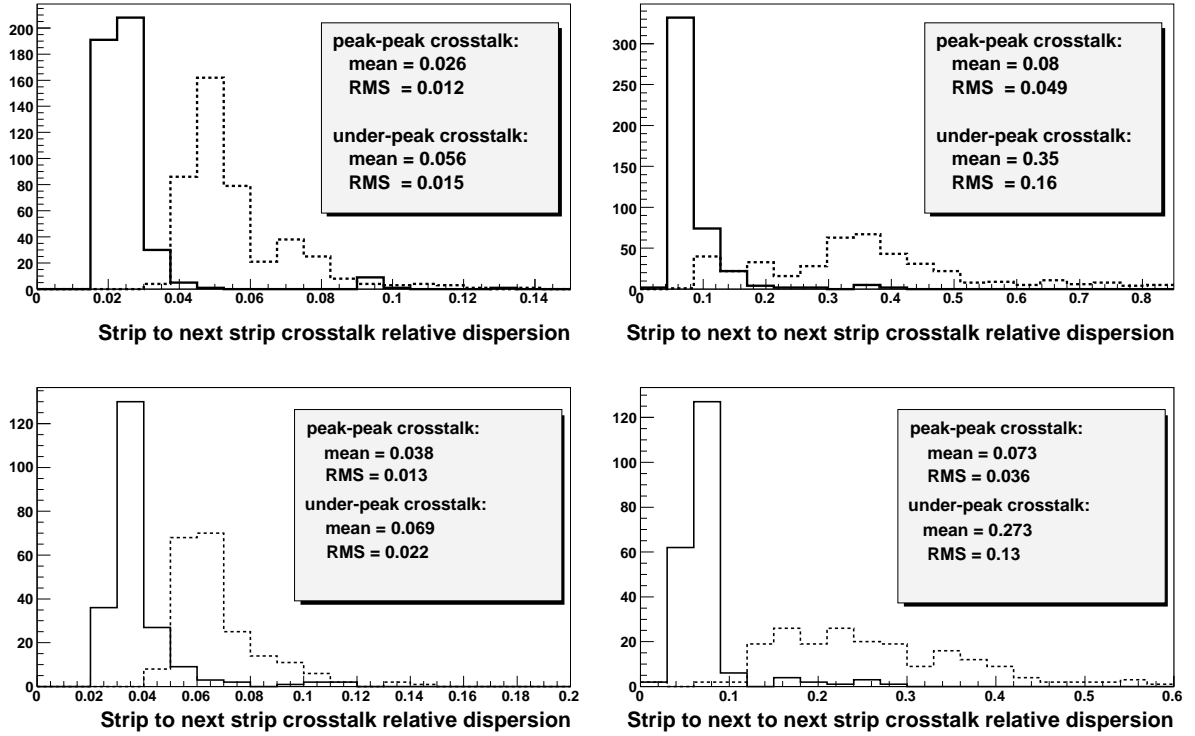


Figure 5: Distributions of the ratio of the RMS to the mean for each Φ -value in the barrel (top) and endcaps (bottom). Right: strip to neighbour strip crosstalk, left: strip to next to neighbour strip crosstalk. In plain line the peak-peak definition was applied, whereas the under-peak definition is shown in dashed line.

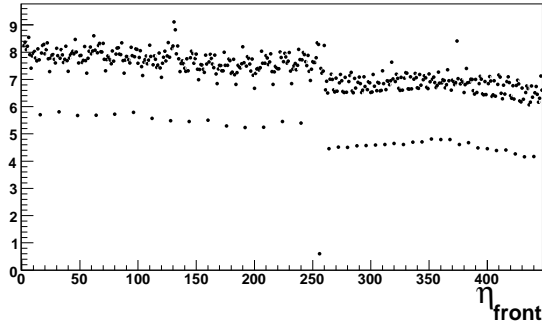
The rest of the front cells gradually change their size so that with η the capacitance C_x changes from 60 pF to 30 pF, while the detector capacitance C_d varies from 90 to 160 pF. As calculated from the schematics shown in Figure 3 [1] this provides a decrease of the peak-peak crosstalk values from 10% to 6% (5% to 2% for under-peak crosstalk).

2.2.2 Strip to next to neighbour strip crosstalk

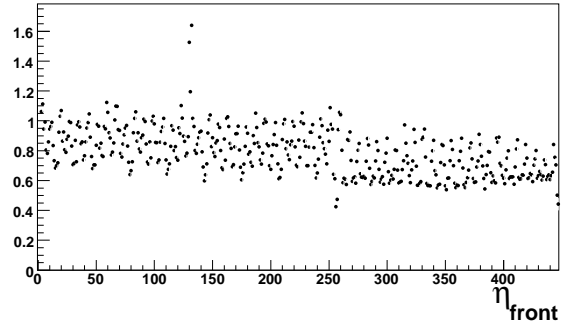
The strip to next to neighbour strip peak-peak crosstalk ranges in the barrel between 0.6 and 1.1 % ($< 0.6\%$ for under-peak crosstalk) and in the endcap between 0.5 and 1 % (resp. $< 0.5\%$). Its dependence with η can be found in Figures 6 and 7.

The first four cells in the endcap front layer have calibration patterns different from the rest of the cells in that sampling; every second cell is pulsed, instead of every fourth, as shown in annex A. Therefore, next to neighbour crosstalk values extracted from the standard calibration scheme are omitted.

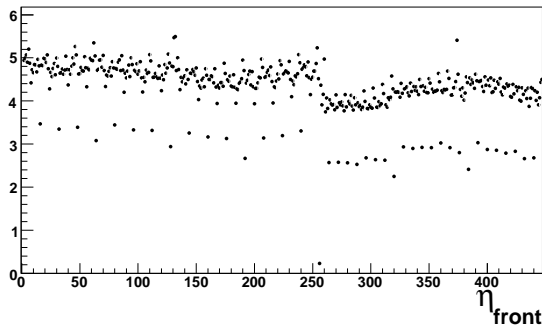
Front layer : strip to next strip peak-peak crosstalk (%)



Front layer : strip to next to next strip peak-peak crosstalk (%)



Front layer : strip to next strip under-peak crosstalk (%)



Front layer : strip to next to next strip under-peak crosstalk (%)

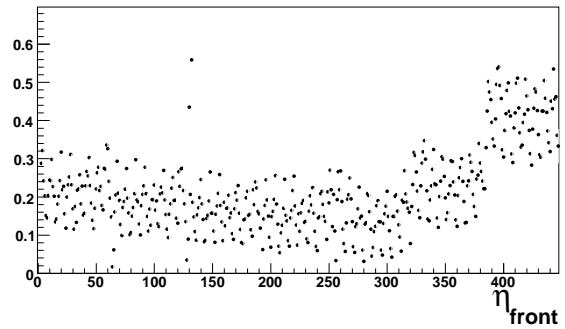


Figure 6: Front layer crosstalk in the barrel averaged in Φ as a function of channel number along η . On the top are shown peak-peak crosstalk values between neighbour channels (left) and next-to-neighbour channels (right). On the bottom there are under-peak crosstalk values between neighbour channels (left) and next-to-neighbour channels (right).

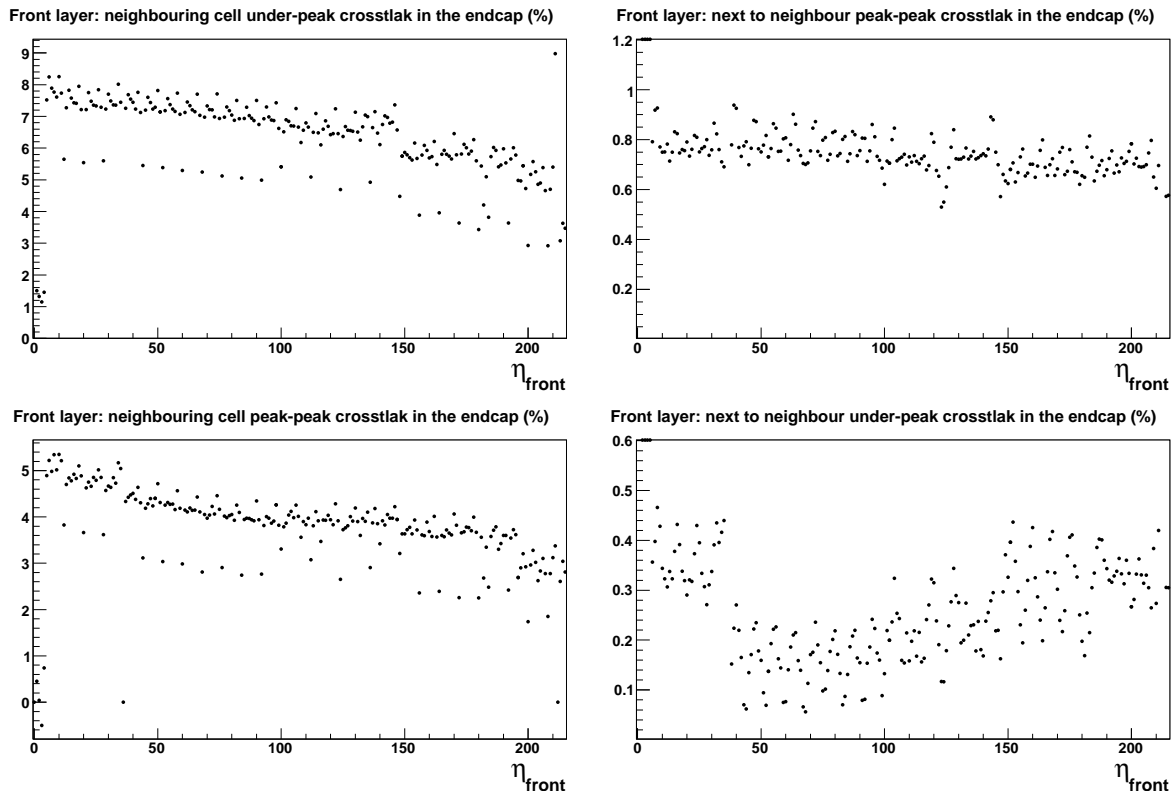


Figure 7: Front layer crosstalk in the endcap averaged in Φ as a function of channel number along η . On the top there are shown peak-peak crosstalk values between neighbour channels (left) and next-to-neighbour channels (right). On the bottom there are under-peak crosstalk values between neighbour channels (left) and next-to-neighbour channels (right).

3 Resistive Crosstalk between Middle and Front Samplings

3.1 Origin

The high voltage (HV) is supplied to the front sampling by ink resistors that physically connect cells to the medium sampling: the resulting resistive crosstalk is dominant between these two layers. This section focuses on crosstalk in the front sampling when the middle sampling is pulsed.

In Figure 8 the equivalent schematic of the HV resistors on the kapton electrode is shown. The calibration pulse V_{cal}^M is applied to the middle sampling via the injection resistors R_{cal}^M and part of the signal flows to the front sampling through the resistors R_{M-F} (hundreds of $k\Omega$). The crosstalk value is proportional to the inverse of the resistance cal-

culated for parallel-connected resistors that are located in the front of the pulsed middle cell [1]. For purely resistive crosstalk no dephasing is introduced between the pulsed middle cell and the neighbouring front cell: in this case peak-peak and under-peak crosstalk are equivalent.

In addition to the purely resistive coupling, the middle-front crosstalk is affected by long distance crosstalk between these two layers. Long distance crosstalk can be observed and quantified in a front sampling cell when a calibration signal is sent to a middle layer channel which is not connected to the mentioned front channel. However, the contribution of this type of crosstalk is minor compared to the resistive type (see figure 9). In this study the full middle sampling to front sampling neighbourhood crosstalk was measured.

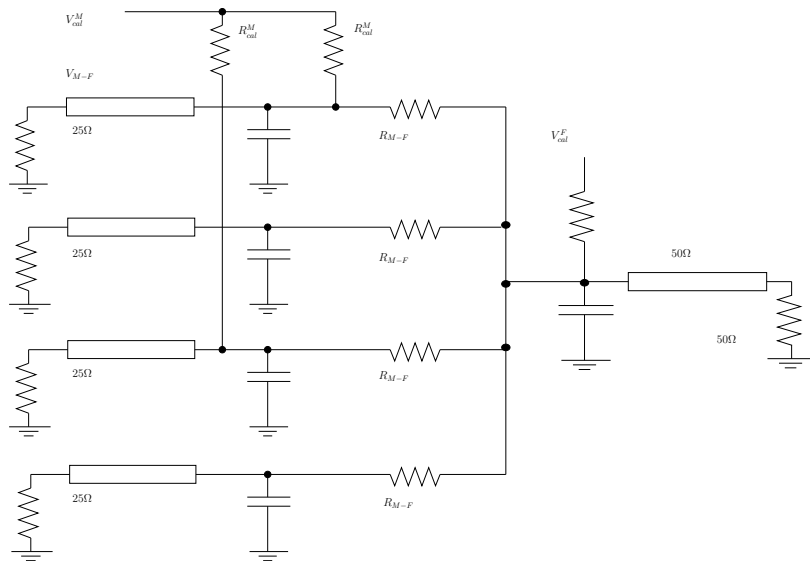


Figure 8: Equivalent schematic of the HV resistor on the kapton electrode.

3.2 Measurement

Middle to front samplings crosstalk values for 2008 data are summarized in Table 2 and compared with previous measurements done during the test beam. In the barrel the crosstalk values are different for each electrode (see below), so results are show for both of them independently. The overall agreement is reasonable, the minor discrepancy is probably due to the long distance crosstalk correction applied in previous analysis so that the two crosstalk definitions are equivalent in the test beam results.

The middle to front samplings crosstalk as a function of η is shown in figure 11. In this figure the peak-peak definition was used (under-peak crosstalk the results are very close). The crosstalk is uniform along ϕ and the relative dispersion along ϕ direction is close to 15 %. The distribution of the relative dispersion (ratio for each value of Φ of the RMS to the mean) is shown in figure10.

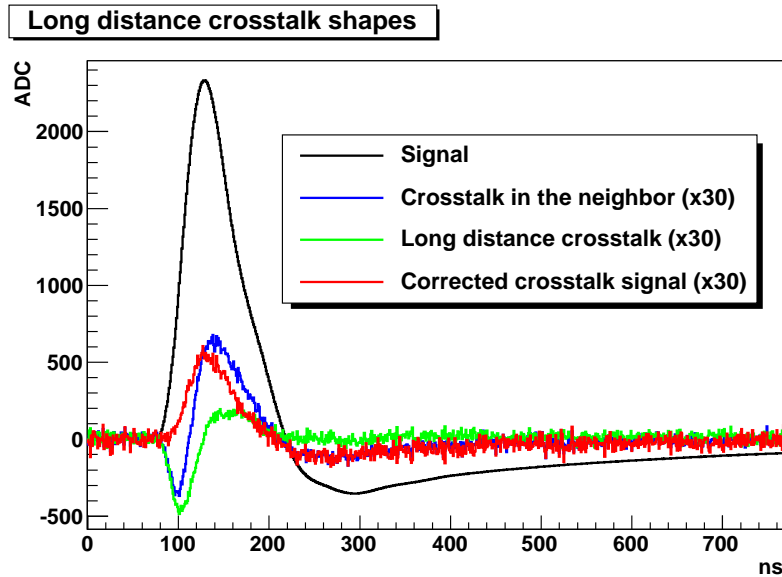


Figure 9: Middle to front samplings crosstalk shapes. In black is the pulsed middle channel. In blue is the crosstalk in a front layer cell which is next to the pulsed one. In green is the long distance crosstalk. The shape in red is the long distance crosstalk subtracted from the middle-strip crosstalk. Crosstalk signals are scaled by a factor 30.

Crosstalk type	Barrel		Endcap
	Electrode A	Electrode B	
Peak-peak crosstalk	0.089 %	0.099 %	0.097 %
RMS	0.013 %	0.022 %	0.022 %
Under-peak crosstalk	0.070 %	0.093 %	0.077 %
RMS	0.014 %	0.022 %	0.015 %
Test beam measurements	0.05 %	0.16 %	0.18 %

Table 2: Middle to front samplings peak-peak and under-peak crosstalk present (2008) results compared with the previous (1999 and 2001-2002 test beam [2][5]) pure resistive crosstalk measurements.

In the barrel, the crosstalk ranges between 0.08 and 0.11 % in electrode A and between 0.08 and 0.16 % in electrode B. Two sets of resistances have been used inducing higher crosstalk in electrode B. The increase of the crosstalk with respect to η is correlated with the decrease of the resistances values. In the endcap the crosstalk ranges between 0.06 and 0.15 %. The dips every 8 channels in the barrel and every 8/6/4 channels in the endcap (depending on the granularity) are due to larger resistances in the first and last

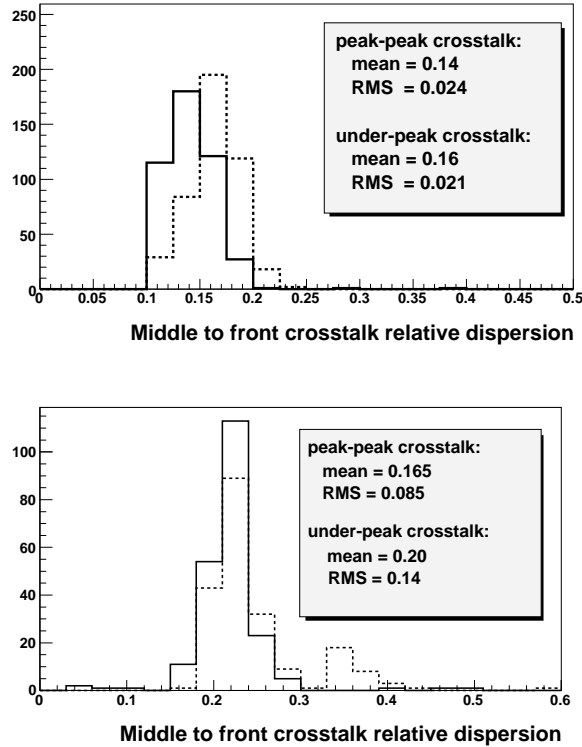


Figure 10: Middle sampling to front sampling crosstalk: distributions of the ratio of the RMS to the mean for each Φ -value in the barrel (top) and the endcap (bottom). In plain line the peak-peak definition was applied, whereas the under-peak definition is shown in dashed line.

front sampling cell of the group facing the middle cell, which make lower the crosstalk value.

4 Inductive Crosstalk in Middle and Back Samplings

4.1 Origin

In the middle and back samplings the main source of crosstalk is mutual inductance between the cells and from the ground return [1]. The capacitive coupling on the electrodes themselves is negligible for these layers. The localization of cells affected by the crosstalk is not well defined in this case, and we choose to keep looking at the next in η neighbour cell for crosstalk inside the sampling, or the cells in front of the pulsed one for inter-layers crosstalk. This choice provides a reasonable estimate of the mean crosstalk value and is

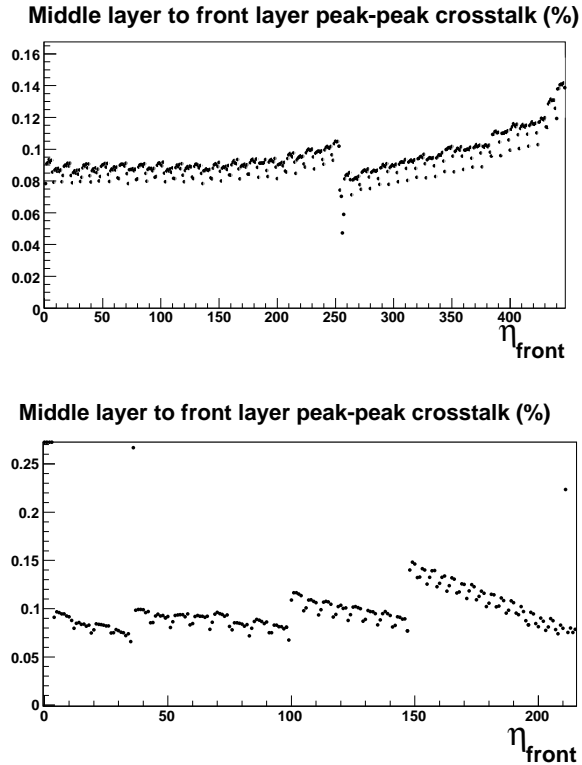


Figure 11: The η dependence of the middle to front layer peak-peak crosstalk averaged in Φ in the barrel (top) and in the endcap (bottom).

similar to energy reconstruction that associates neighbouring cells.

This section is focused on crosstalk inside and between middle and back samplings (middle to middle, middle to back and back to back crosstalk). Typical shapes can be seen in Figure 12 for the cell neighbouring next in η or in front of the pulsed cell.

4.2 Measurement

The crosstalk values estimated in 2008 for the middle and back layers are given in Table 3 and compared to the 2000-2002 test beam measurements performed after the redesign of the motherboards, which has lowered down the inductive crosstalk [3]. For the endcap back layer channels the presented results are for the crosstalk between the channels that share the same summing boards connector (see below). The worse agreement for under-peak crosstalk comes from the large time sensitivity of this type of crosstalk. The η dependence of each type of crosstalk is treated in the following paragraphs.

The η dependence of back sampling cell to back sampling cell crosstalk is shown in figure 16. In the endcap there is a systematic dip every second channel: it corresponds to lower coupling between channels that do not belong to the same summing board connector.

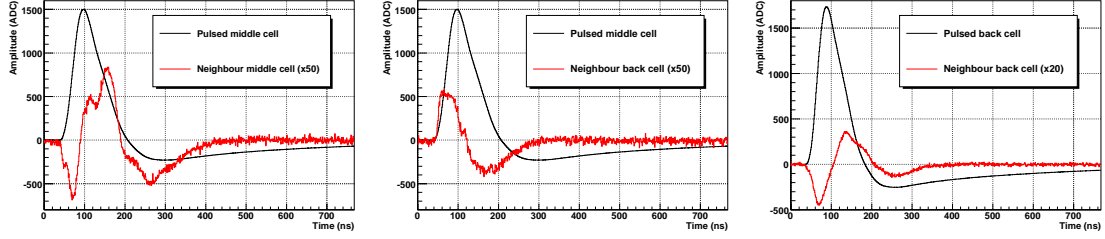


Figure 12: Middle sampling cell to middle sampling cell (left), middle sampling cell to back sampling cells (centre) and back sampling cell to back sampling cells (right) crosstalk shapes (in red). The pulsed cell is displayed in black and the crosstalk wave shapes are magnified.

Crosstalk type	Barrel		Endcap	
	peak-peak	under-peak	peak-peak	under-peak
Middle to middle	1.11 %	0.44 %	0.63 %	-0.24 %
RMS	0.32 %	0.26 %	0.31 %	0.40 %
Test beam measurements	1.7 %	0.85 %	0.9 %	< 0.2 %
Middle to Back	0.88 %	0.61 %	1.17 %	0.034 %
RMS	0.32 %	0.18 %	0.56 %	0.59 %
Test beam measurements	0.9 %	0.36 %	1.27 %	0.3 %
Back to back	1.43 %	- 0.52 %	3.37 %	-1.15 %
RMS	0.52 %	0.28 %	0.42 %	0.85 %
Test beam measurements	1.6 %	0.68 %	3.1 %	0.7 %

Table 3: Middle cell sampling to middle cell sampling, Middle cell sampling to back cell sampling and back cell sampling to back cell sampling crosstalk results compared with the previous test beam measurements [3][5].

This explains why the crosstalk is very different for odd and even η channels. The same phenomena can be seen in the barrel but it is not as significant as in the endcap. The signal and crosstalk shapes are shown in figure 13.

The η dependence of middle sampling cell to middle sampling cell and back sampling cell crosstalk can be seen respectively in figures 14 and 15. The change of electrode in the barrel and the different regions in the endcap is clearly visible. In the barrel this change occurs at $\eta = 16$ for the back and $\eta = 32$ for the middle layers, in the endcap it occurs in the central region ($1 < \eta < 19$ in the back, $6 < \eta < 39$ in the middle layer), and the edges. In the endcap the different regions are pulsed and read out by the electronic boards located in the different types of crates. This explains why there is no data for cells with $\eta = 1$ and $\eta = 20$ in the back and $\eta = 0$ and $\eta = 40$ in the middle layer: since they are in different partitions, the neighbour channels are not read-out when the pulsed channels

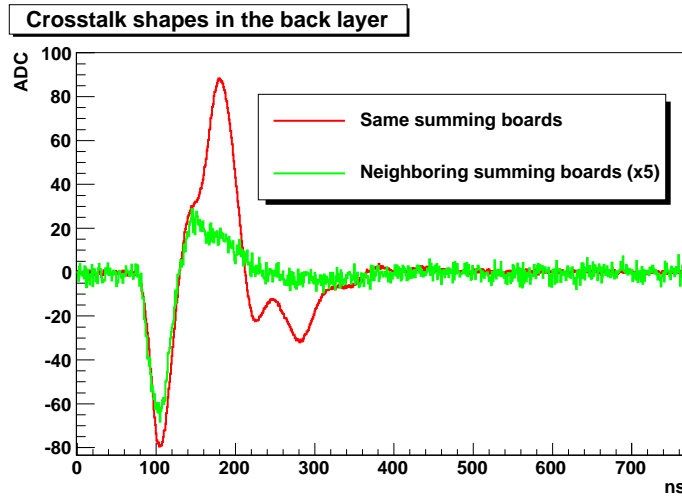


Figure 13: Inductive crosstalk signals in the endcap back layer between cells from the same and from the neighbour summing boards.

get the signal. The high crosstalk value of the last four cells in the middle endcap layer is explained by the absence of the ground return on the electrode connector at low radius. Both in the barrel and in the endcap the effect of channels that are adjacent in the same summing board connector, or simply belong to the same summing board connector, is present, although it is not as predominant as in the case of the endcap back sampling cell to back sampling cell crosstalk.

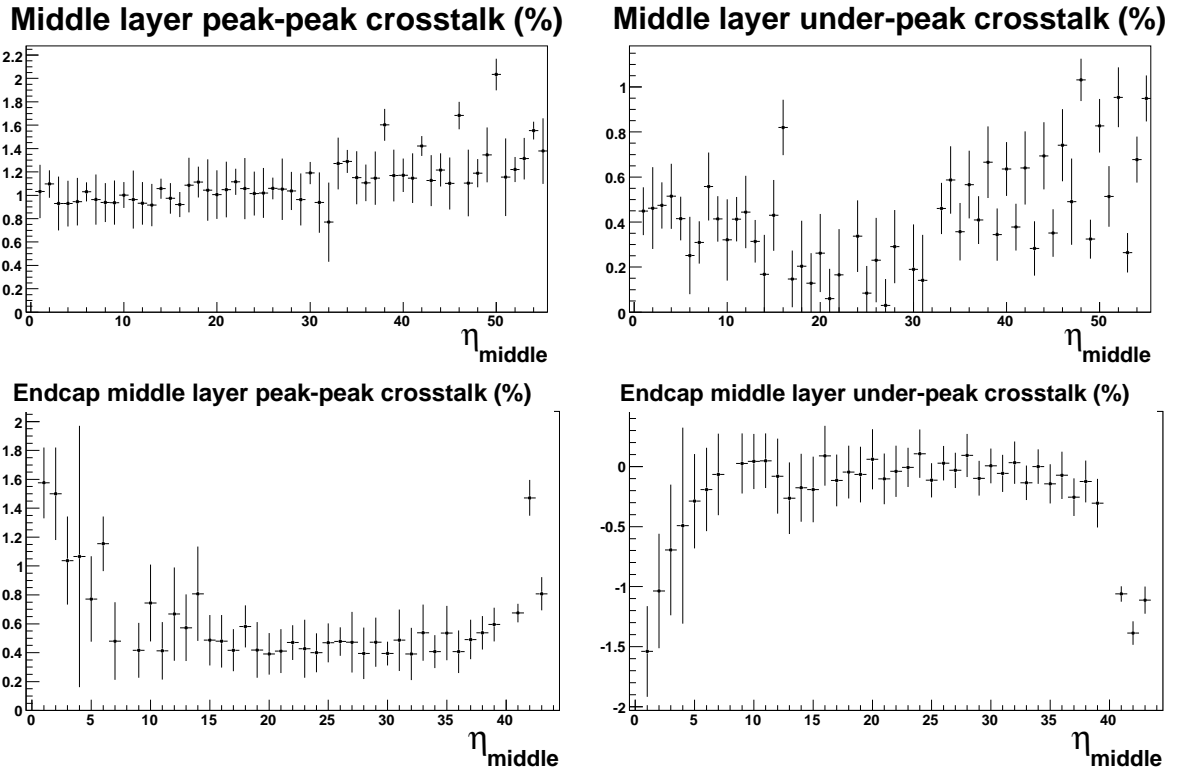


Figure 14: The η dependence of the middle sampling cell to middle sampling cell peak-peak (left column) and under-peak (right column) crosstalk in the barrel (top) and the endcap (bottom).

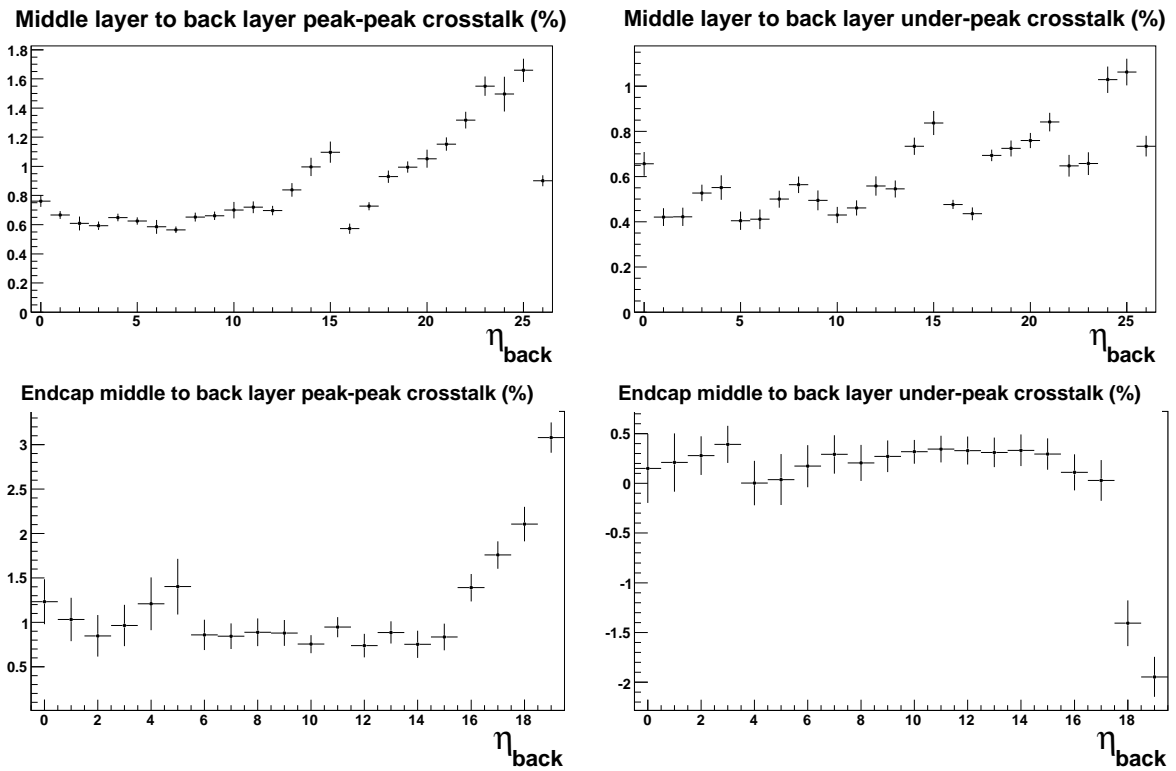


Figure 15: The η dependence of the middle sampling cell to back sampling cell peak-peak (left column) and under-peak (right column) crosstalk in the barrel (top) and the endcap (bottom).

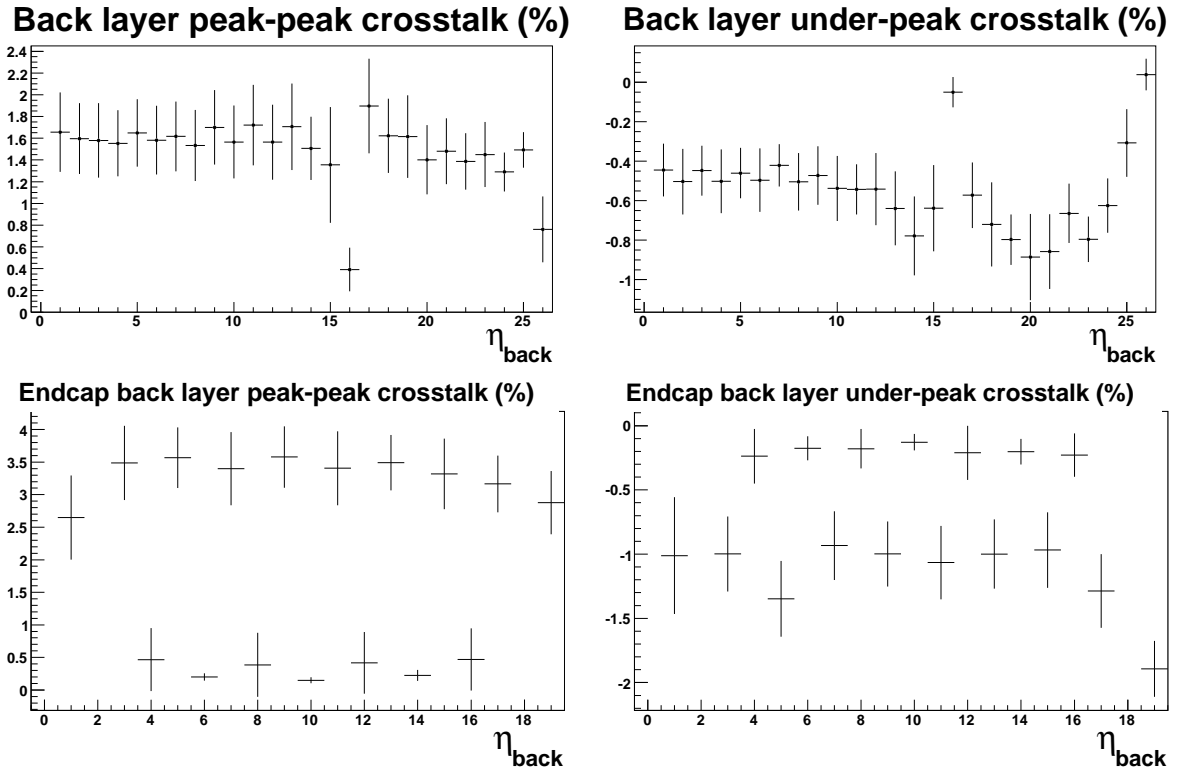


Figure 16: The η dependence of the back sampling cell to back sampling cell peak-peak (left column) and under-peak (right column) crosstalk in the barrel (top) and the endcap (bottom).

5 Crosstalk Analysis as Tool to Characterise Misbehaving Channels

5.1 Introduction

Noise, delay or ramp studies are good ways to find misbehaving channels. Crosstalk analysis gives some useful additional information that helps classify them:

- The crosstalk computation needs the wave shape reconstruction of non-pulsed channels, which is a relevant observable for misbehaving channels.
- As the crosstalk reflects the relation between two channels, its analysis is a good way to investigate pathological interactions between two channels.
- Crosstalk measurements between layers allow the detection of some channel inversions, in particular along Φ where behaviors are in general uniform.

Consequently, crosstalk analysis is particularly relevant to the study of dead or distorted channels, shorts and channels inversions. List of analyzed misbehaving channels can be found in annex B.

5.2 Dead and distorted channels

In calibration, pulses come from the calibration boards, located in the front end crates, to the motherboards in the cryostat. The motherboards distribute the pulses to the calorimeter cells corresponding to the calibration pattern described in annex A through injection resistors, and send the output signal to the reading chain [8].

In calibration runs, a channel is considered as dead if no signal or a very low amplitude is read. A priori there could be three types of dead channels: dead at the level of calibration chain, read-out chain or in physics. Crosstalk studies should distinguish between them. In the same way the cause of misbehavior for distorted channels or channels with bad shape can be analyzed with crosstalk. The list of analyzed dead or distorted channels can be found in annex B.1. Some of them may affect their neighbourhood (for example with large, long or oscillating crosstalk) and this feature is visible in crosstalk analysis when the bad cell is pulsed. Those “leaking” channels may be harmful (see, for example, the case of the generous leaking dead channels below), and in this case should be taken into account in energy reconstruction.

5.2.1 Dead calibration channels

In this case the calibration line is affected but the readout chain should still be operational; even if the cell can not be calibrated it may be used with a physical signal coming from liquid argon ionization. This means that in calibration runs the crosstalk signal of a dead calibration channel should not be affected when its neighbours are pulsed. The channel appears dead only when its corresponding calibration pattern is pulsed.

The problem could occur in the calibration line between the calibration board and the motherboard, before the signal splits into the different channels of the calibration pattern; in this case all the channels of the pattern are dead. The second possibility is a problem at the level of the injection resistor after the splitting. In this case only a single channel is affected.

5.2.2 Dead readout channels

If the readout chain of a channel is dead, the channel is lost: no signal can be read in physical or calibration runs. This feature can be analyzed in calibration runs using crosstalk measurements, because the channel appears dead even if the neighbour cell is pulsed. Some dead readout channels are leaking channels as in the case of “generous” leaking dead channels studied below.

Generous leaking dead channels Generous leaking dead channels are a particular case of those dead channels that affect their neighbourhood. It happens in the front layer and is very dramatic since about 20 % of the pulse applied at the dead front sampling cell is transferred, not derived, to each of its two neighbours.

This could be explained by a lack of ohmic contact through the preamplifier chain. Indeed, the theoretical crosstalk current between two neighbour front cells [1] in the frequency s domain is given by :

$$I_x = \frac{sC_x R_{in}}{1 + s(C_x + C_d)R_{in}} \times I_d$$

where I_d is the current injected by the calibration board, C_x and C_d are respectively the crosstalk and detector capacitance, R_{in} the preamplifier input impedance of the pulsed channel, and where the approximation that C_x is small in comparison with C_d has been used. With a lack of ohmic contact through the preamplifier chain ($R_{in} \rightarrow \infty$) the pulsed channel becomes dead (no signal measured) and the neighbour crosstalk current becomes:

$$I_x = \frac{C_x}{C_x + C_d} \times I_d$$

simply proportional to the injected current, therefore there is no derivation. The factor $\frac{C_x}{C_x + C_d} \simeq 25\%$ with the typical values of capacitance found in the front layer ($C_d \simeq 150$ pF and $C_x \simeq 50$ pF [1]) which is close to the 20 % observed. This seems to be confirmed by the campaign of electrical measurements made during calorimeter integration in 2003-2004, in which all the found generous leaking dead channels present a calibration channel open (infinite calibration resistance) [7].

5.2.3 Dead in physics channels

The third case involving dead channels is that in which the cell is disconnected from the motherboard, and could therefore be called a dead “physics” channel. Since, for

calibration, the current is injected by the calibration boards in the motherboard at the input of the cell, those channels should not appear as “dead” in calibration runs. However, the disconnection of the physical cell from the readout electronics should imply a lower peaking time, a higher amplitude [4] and the disappearance of the crosstalk due to the detector (mainly resistive and capacitive types). This type of dead channel has to date never be observed in this study.

5.2.4 Distorted channels

As for dead channels, crosstalk studies help to distinguish between calibration or readout origin for distorted channels or channels with bad shapes. In this case these channels could be used in physical measurements, the relevant question is which calibration constants should be used. If the channel is distorted due to the readout chain (same misbehavior when other channels are pulsed) one should use in physical runs the calibration constants computed for this channel in calibration runs. If the cause of the distortion is the calibration chain (strange behavior observed only when the misbehaving channel is pulsed), relevant calibration constants can be estimated using the azimuthal symmetry of the calorimeter, since in this case the readout chain is probably not affected. A list of distorted channels and channels with bad shapes, analyzed with crosstalk observations, is given in annex B.1.

5.3 Shorts

Crosstalk analysis is particularly relevant to finding and analyzing shorts since these pathologies affect the link between two channels. On the electrodes themselves, a short could occur either in the signal layer or in the high-voltage layer. In fact, since the summing boards are passive electronics, even if each cell is the sum along Φ of many electrodes a short on only one layer affect the whole cell. A list of shorts and their classification can be found in annex B.2.

5.3.1 Short in signal layer

A short in signal layer is characterized by a purely resistive crosstalk (of 100 % for perfect shorts).

5.3.2 Short in high voltage layer

A short in the high voltage layer induces an additional crosstalk capacitance between the two channels corresponding to the two high voltage capacitances (kapton capacitance) in serial, that is a capacitance of $C'_x = C_{HV}/2$ where C_{HV} is the kapton capacitance [2]. For example, in the front layer where the crosstalk is mainly capacitive ($C_X \sim 50\text{pF}$), a short in the high voltage layer ($C_{HV} \sim 200\text{pF}$) yields a crosstalk around 15 %.

5.4 Channels swapping

The calibration chain is designed in such way that it pulses simultaneously several channels. Therefore, a single check of the pulsed channels output is not enough to fully validate the cabling of the readout chain. Some remaining ambiguities can be removed by performing crosstalk analysis.

Two types of inversions were found in the front layer: inversion of two Φ regions of the same front end board (FEB) and inversion of two motherboard connectors. These two cases are described below, after review of the cabling scheme between the motherboards and the FEBs. The observed cabling mistakes are listed in annex B.3.

The problems were fixed on both readout chains: the analog level 1 (L1) trigger and the main digital one.

5.4.1 Cabling from motherboards to the front end boards

The signal is read out from the motherboards via the low profile receptacles in groups of 8 channels (for the barrel). The A harness is plugged into the low profile connectors with a μ -D connector grouping 64 channels, which correspond to one of the two Φ regions ($\Delta\eta \times \Delta\Phi = 0.2 \times 0.1$) of each FEB. The A harness is going to the module patch panel. From the patch panel a second harness (B harness) brings the signal to the feed-through cold flange via an ATI connector (64 channels). Finally, a warm cable of 64 channels connects the feed-through warm flange to the base-plane where the front-end boards are plugged [8].

5.4.2 Motherboard connectors swapping

Very low values of middle sampling to front sampling crosstalk in sixteen consecutive channels in the front layer were explained by inversion of two motherboard connectors. Analysis of the amplitudes in the front layer when the middle layer channel is pulsed shows inversion of two groups of eight channels (each middle sampling cell being in front of eight front sampling cells). This was fixed by re-swapping the channels in the cabling software database for the main readout. This didn't affect the L1 trigger, since the sixteen affected channels are located in the same trigger tower.

5.4.3 Front-end board Φ -regions swapping

Analysis of the amplitudes of front layer channels, which have very low crosstalk values when the neighbouring middle layer channels is pulsed, reveals the swapping of the Φ -regions of the FEB, that is, the swapping of the two groups of channels $0 \rightarrow 63$ and $64 \rightarrow 127$. This means swapping either one of two harnesses B or one of two warm cables. Considering that the warm cables are not flexible enough to be swapped, the mistakes are probably at the level of the patch panel.

One possible fix of the problem is to swap two warm cables (patch panels are no longer accessible). But this leads to the realization of dedicated cables and requires removal of the

crate and base-plane. This also generates a risk of large crosstalk and noise propagation at the crossing of the two cables. For these reasons the suggested fix for this inversion is to re-swap the channels in the software cabling database. In this case the two Φ -regions are not located in the same trigger tower ($\Delta\eta \times \Delta\Phi = 0.1 \times 0.1$): to restore the correct analog signal routing, hardware modifications are needed between the FEB and the trigger tower builder.

This second operation takes place at the level of the layer sum boards. Those components, two per FEB on each side of the Printed Circuit Board, are connected to the Tower Builder Boards through the J2 connector. Each carries the front sampling for its Φ -region: the fix, consequently, is to swap the outputs of the two layer sum boards. This has been done by using the Printed Circuit Board through-holes.

5.5 Summary

Problematic channels analyzed in the crosstalk studies are summarized in Table 4. For details on problems found in the barrel see the link [10], in the endcap see the link [11].

Number of problems:	Barrel	Endcap
Dead channels because of the calibration chain	26	6
Dead channels because of the readout chain	14	12
Distorted channels because of the calibration chain	25	27
Distorted channels because of the readout chain	11	27
Leaking channels	12	13
Shorts in the signal layer	2	0
Shorts in the high voltage layer	2	0
Front-end board Φ -regions swapping	3	0
Motherboard connectors swapping	4	0

Table 4: Types of problems found during the crosstalk studies.

6 Conclusion

Crosstalk values inside the liquid argon calorimeter have been measured at the ATLAS final installation stage in 2008. These values are summarized in table 5. They are compatible with previous test beam measurements, meaning that the whole detector crosstalk behaves as expected based on previous modules studies.

The crosstalk study is useful in the taxonomy of misbehaving channels. It helps especially to characterize dead or distorted channels, shorts and to find channel inversions.

Crosstalk type	Barrel		Endcap	
	peak-peak	under-peak	peak-peak	under-peak
Capacitive crosstalk				
Strip to neighbour strip	7.16 %	4.34 %	6.33 %	3.8 %
RMS	0.90 %	0.60 %	1.1 %	0.67 %
Strip to next to neighbour strip	0.78 %	0.22 %	0.89 %	0.40 %
RMS	0.17 %	0.12 %	0.10 %	0.12 %
Resistive crosstalk				
Middle to front sampling	0.096%	0.082%	0.097%	0.077%
RMS	0.018%	0.018%	0.022%	0.015%
Inductive crosstalk				
Middle to middle sampling	1.11 %	0.44 %	0.63 %	-0.24 %
RMS	0.32 %	0.26 %	0.31 %	0.40 %
Middle to back	0.88 %	0.61 %	1.17 %	0.034 %
RMS	0.32 %	0.18 %	0.56 %	0.59 %
Back to back sampling	1.43 %	- 0.52 %	3.37 %	-1.15 %
RMS	0.52 %	0.28 %	0.42 %	0.85 %

Table 5: Summary of 2008 crosstalk measurements.

Acknowledgements

We would like to acknowledge the whole LAr calorimeter commissioning community for their feedback, their technical explanations, and their useful ideas to understand or fix some of the strange behaviours seen in the calorimeters. We are in particular very grateful to Benjamin Trocmé (LPSC), Emmanuel Monnier (CPPM), Martin Aleksa (CERN), Fabrice Hubaut (CPPM), Laurent Serin (LAL), Stefan Simion (LAL), Bill Cleland (University of Pittsburgh), Daniel Fournier (LAL), Guillaume Unal (CERN), Fabien Tarrade (BNL), Walter Lampl (University of Arizona), Marco Delmastro (CERN), Julia Hoffman (SMU) and Ryszard Stroynowski (SMU).

References

- [1] J. Colas et al., *Crosstalk in the ATLAS Electromagnetic Calorimeter*, ATL-LARG-2000-004.
- [2] F. Hubaut et al., *Test beam Measurement of the Crosstalk in the EM Barrel Module 0*, ATL-LARG-2000-007.
- [3] F. Hubaut, *Crosstalk measurement in the EM barrel module 0 from 99', May 00', and July 00' beam tests*, ATL-LARG-2000-009.
- [4] P. Pralavorio and D. Sauvage *Review of the crosstalk in the module 0 of the Electromagnetic Endcap Calorimeter*, ATL-LARG-2001-006.
- [5] F. Hubaut et al., *Crosstalk in production modules of the electromagnetic endcap calorimeter*, ATL-LARG-2003-012.
- [6] M. Aleksa et al., *2004 ATLAS Combined Testbeam: Computation and Validation of the Electronic Calibration Constants for the Electromagnetic Calorimeter*, ATL-LARG-PUB-2006-003.
- [7] D. Lacour and P. Perrodo *Electrical tests on the ATLAS barrel electromagnetic liquid argon calorimeter*, ATL-LARG-INT-2005-003, ATL-COM-LARG-2005-008.
- [8] C. Cerna et al., *Cabling of the ATLAS liquid argon calorimeters*, ATL-A-EN-0001.
- [9] See the presentation given by Marumi Kado at the EM general meeting, CERN, the 23 March 2004.
- [10] <http://lpsc.in2p3.fr/atlas/labbe/BP3C/Xtalk/pathology.php>
- [11] <https://twiki.cern.ch/twiki/bin/edit/Atlas/LArEndcapP3CommissioningXtalkProblems>

A Calibration patterns

Figures 17 and 18 show the calibration patterns applied on the electromagnetic calorimeter. In order to retrieve the situation where only one cell is pulsed the following factor have been applied to the crosstalk computation :

- In front the layer, for the strip to next neighbour strip crosstalk : every channel has two next to neighbour channels that are pulsed at the same time during a calibration run. Apply a factor 0.5.
- Middle sampling to front sampling crosstalk : any front sampling cell has two middle sampling cells pulsed simultaneously next to it. Apply a factor 0.5.

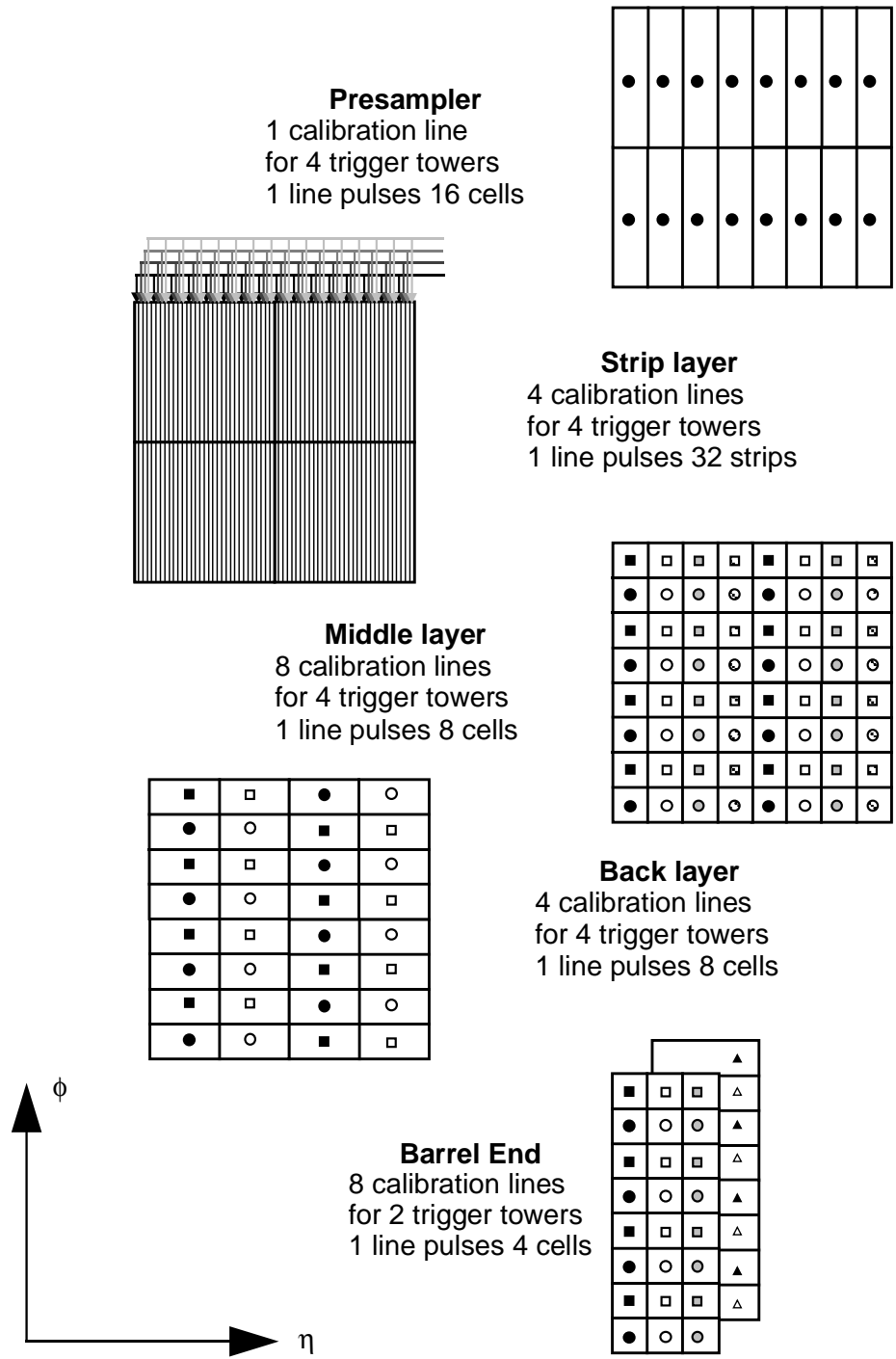


Figure 17: Symbolic representation of the calibration pattern in the electromagnetic barrel calorimeter. Within a given depth layer, calibration lines with common symbol are pulsed simultaneously.

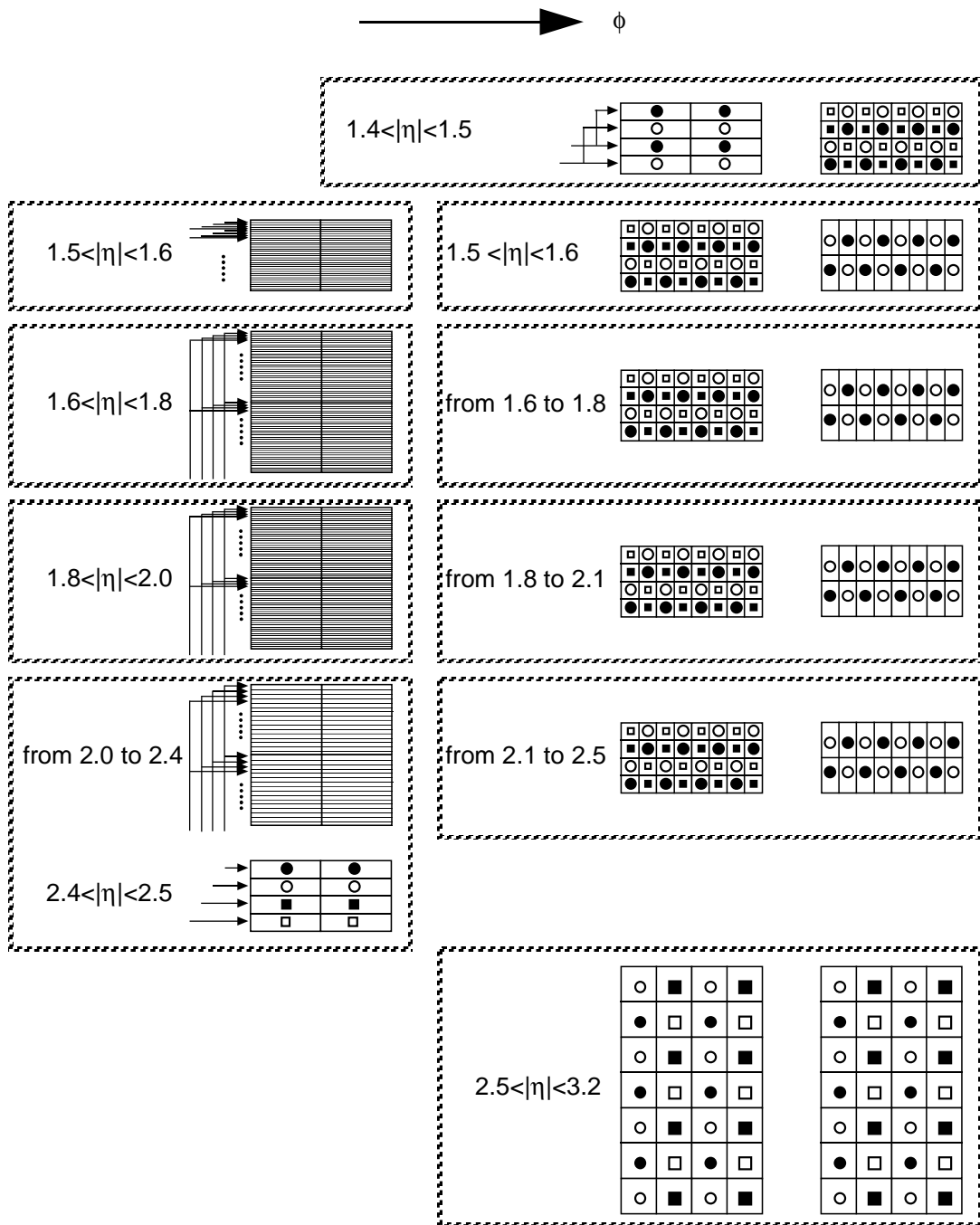


Figure 18: Symbolic representation of the calibration pattern in the electromagnetic endcap calorimeter. Each cross-hatched box represents a motherboard. In the front layer (left), strips which are pulsed simultaneously are indicated by connected lines. In the middle and back layers (right), calibration lines which are pulsed simultaneously (within a given depth layer) are indicated by a common symbol.

B Misbehaving channel list

B.1 Dead or distorted channels

Known dead and distorted channels have been analyzed with crosstalk, and compared with reference waveshapes. These reference waveshapes have been taken in the same η -position as the considered channel using the symmetry of the detector along the ϕ direction. The tagging has been done as follows:

- If the channel pulsedshape amplitude deviates more than 5 standard deviation from the reference,
 - Then if the crosstalk waveshape amplitude of the above channel also deviates more than 5 standard deviations from the reference when its neighbour cell is pulsed a “Readout origin” tag is applied (channel misbehaving in any cases).
 - Else, a “Calibration origin” tag is applied (channel misbehaving only when pulsed).
- If, when the channel is pulsed, its neighbour get a crosstalk signal greater than 5 standard deviations from the reference, a “Leaking” tag is applied.

Analyzed dead channels are summarized in table 6 page 31 for the half-barrel A, in table 7 page 32 for the half-barrel C, and in table 8 page 34 for both endcaps. Analyzed distorted channels in both half-barrels are given in the table 9 page 35. Distorted channels in the endcap are summarized in the table 10 page 36 for the endcap A and in the table 11 page 37 for the endcap C. The waveshapes of the main leaking channels can be seen on figure 19 page 33. The particular case of the generous leaking dead channels discribed in section 5.2.2 has been observed for the following channels:

Det.	Side	Crate	FT	FEB	Slot	Channel	Calibration line
EMB	A	I14	26	F1	3	107	19
EMB	C	H04	9	F3	5	71	51
EMB	C	H04	10	F2	4	83	35
EMB	C	H01	15	F3	5	119	51

B.2 Shorts

The observed shorts in the barrel are given in table 13 on page 38.

B.3 Channel swapping

The observed channels swapping, as discribed in the section 5 are given in table 12 on page 37.

B.4 Other crosstalk problems

The other seen crosstalk problems are given here:

Det.	Side	Crate	FT	FEB	Slot	Comments
EMB	A	I06	10	B1	10	Long, noisy crosstalk when calibration line 111 pulsed. Associated channels pulse-shapes are distorted.
EMB	C	H06	6	M2	13	Large crosstalk between calibration lines 88 and 89. Associated channels pulseshapes are distorted.
EMB	C	H12	26	M3	14	Large crosstalk in calibration line 105 when calibration lines 100-104 pulsed.
EMB	C	H11	28	M1	12	Many channels problem: large/long crosstalk between channels 59, 61, 62 and 63. The pulseshapes of these channels are distorted.
EMEC	A	2R	2	M1	11	Channel 14 is distorted. It receives large crosstalk signal, but only if not it's neighbours are pulsed, but one of the channels pulsed by calibration line 36
EMEC	A	5R	4	F5	7	Channels 1 and 3 exchange signal: when one of these channels is pulsed, another one gets 100 ADC amplitude crosstalk (average normal is 20)
EMEC	A	7L	12	F5	7	Channel 84 looks like dead both in physics and in calibration
EMEC	C	6R	2	F1	10	Channels 35 and 36 exchange signal: when one of them is pulsed, another one gets 100 ADC amplitude crosstalk (average normal is 20)
EMEC	C	3R	7	B0	8	Large crosstalk between calibration lines 78 and 79. Associated channels pulseshapes are distorted.

Det.	Side	Crate	FT	FEB	Slot	Channel	Calibration line	Comments
EMB	A	I04	6	F5	7	123	83	Readout origin
EMB	A	I04	6	B1	10	54	118	Readout origin, leaking
EMB	A	I05	8	F6	8	111	99	Readout origin, leaking
EMB	A	I05	8	F6	8	115	99	Readout origin, leaking
EMB	A	I06	9	F2	4	1	33	Readout origin
EMB	A	I06	9	F6	8	74	98	Readout origin, leaking
EMB	A	I08	14	B0	9	64	12	Readout origin
EMB	A	I11	20	B1	10	35	109	Calibration origin
EMB	A	I11	20	M3	14	28	107	Calibration origin
EMB	A	I12	21	B0	9	28	0	Readout origin
EMB	A	I12	21	B1	10	115	113	Barrel End channels 112-127 leaking
EMB	A	I12	21	B1	10	117	119	Barrel End channels 112-127 leaking
EMB	A	I12	21	B1	10	118	118	Barrel End channels 112-127 leaking
EMB	A	I12	21	B1	10	119	119	Barrel End channels 112-127 leaking
EMB	A	I12	21	B1	10	121	117	Barrel End channels 112-127 leaking
EMB	A	I12	21	B1	10	123	117	Barrel End channels 112-127 leaking
EMB	A	I12	21	B1	10	125	115	Barrel End channels 112-127 leaking
EMB	A	I12	21	B1	10	127	115	Barrel End channels 112-127 leaking
EMB	A	I14	26	F1	3	107	19	Readout origin, leaking
EMB	A	I15	28	F6	8	115	99	Calibration origin
EMB	A	I00	31	M2	13	23	71	Readout origin, leaking
EMB	A	I00	31	M2	13	126	91	Readout origin, leaking

Table 6: List of the dead channels in the half-barrel A.

Det.	Side	Crate	FT	FEB	Slot	Channel	Calibration line	Comments
EMB	C	H05	7	F5	7	119	83	Calibration origin
EMB	C	H04	9	F3	5	71	51	Readout origin, leaking
EMB	C	H04	10	F2	4	83	35	Readout origin, leaking
EMB	C	H04	10	B1	10	61	115	Calibration origin
EMB	C	H04	10	B1	10	63	115	Calibration origin
EMB	C	H02	14	M2	13	15	70	Readout origin, leaking
EMB	C	H01	15	F3	5	119	51	Readout origin, leaking
EMB	C	H01	16	M1	12	68	42	Calibration origin
EMB	C	H01	16	M1	12	70	42	Calibration origin
EMB	C	H01	16	M1	12	77	42	Calibration origin
EMB	C	H01	16	M1	12	79	42	Calibration origin
EMB	C	H01	16	M1	12	84	42	Calibration origin
EMB	C	H01	16	M1	12	86	42	Calibration origin
EMB	C	H01	16	M1	12	93	42	Calibration origin
EMB	C	H01	16	M1	12	95	42	Calibration origin
EMB	C	H13	24	M2	13	82	72	Calibration origin
EMB	C	H12	26	F4	6	92	64	Calibration origin
EMB	C	H12	26	B0	9	1	13	Calibration origin
EMB	C	H12	26	B0	9	3	13	Calibration origin
EMB	C	H12	26	B0	9	8	13	Calibration origin
EMB	C	H12	26	B0	9	10	13	Calibration origin
EMB	C	H12	26	B0	9	65	13	Calibration origin
EMB	C	H12	26	B0	9	67	13	Calibration origin
EMB	C	H12	26	B0	9	72	13	Calibration origin
EMB	C	H12	26	B0	9	74	13	Calibration origin
EMB	C	H11	28	B0	9	107	44	Readout origin

Table 7: List of the dead channels in the half-barrel C analyzed with crosstalk.

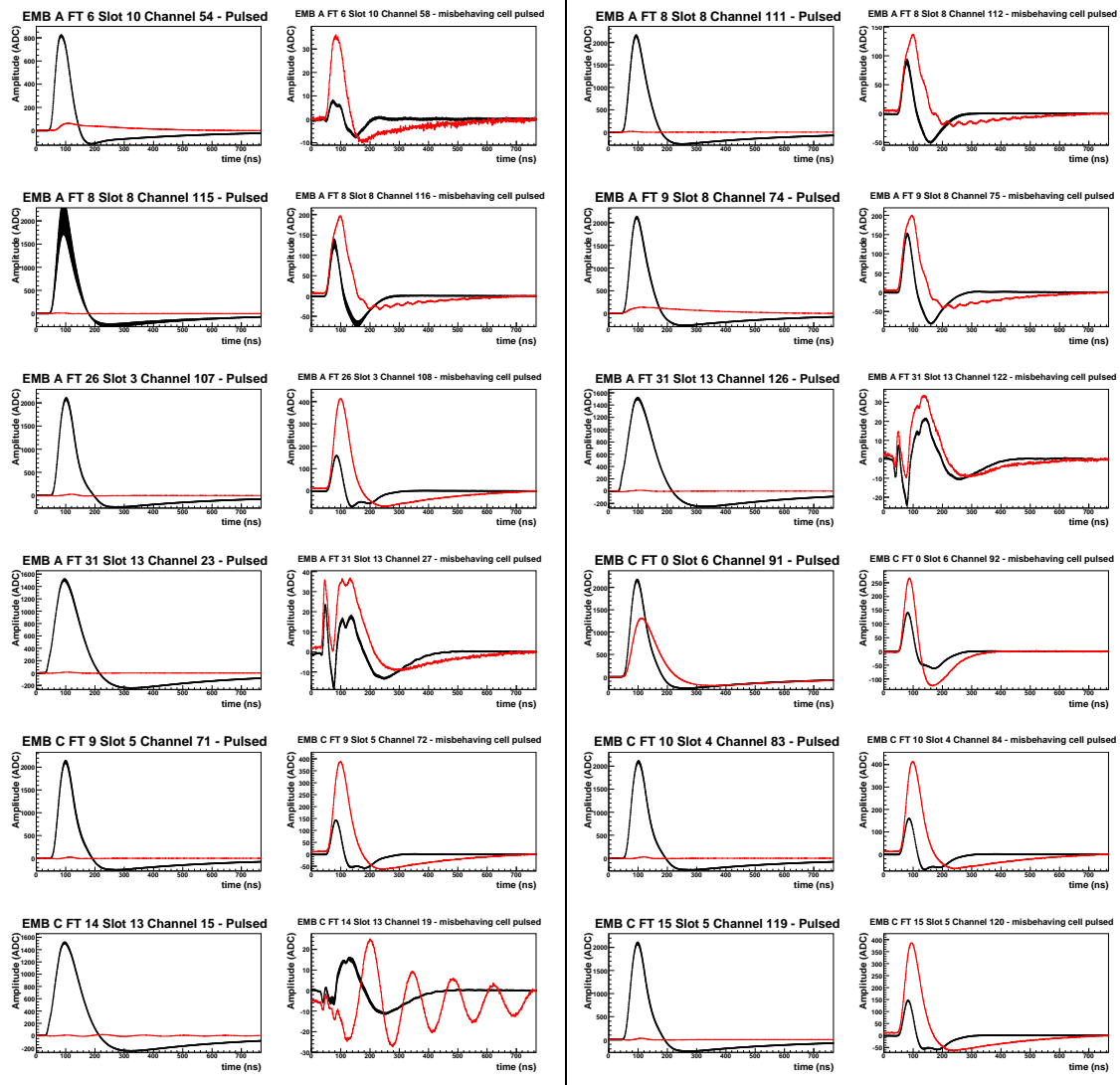


Figure 19: Waveshapes for main leaking channels in the barrel. In each column the first waveshape is the misbehaving cell ones when pulsed, the second is its neighbour ones at the same moment. The studied cells are displayed in red, the reference waveshapes are shown in black.

Det.	Side	Crate	FT	FEB	Slot	Channel	Calibration line	Comments
EMEC	A	1R	0	M3	13	77	54	Readout origin
EMEC	A	2R	2	M1	4	19	3	Calibration origin
EMEC	A	2R	2	F1	5	64	40	Calibration origin
EMEC	A	2R	2	F5	12	27	91	Calibration origin
EMEC	A	2R	2	F5	12	31	91	Calibration origin
EMEC	A	2R	2	B1	13	15	96	Readout origin
EMEC	A	7R	11	M1	11	24	21	Readout origin, leaking
EMEC	A	9R	15	M1	4	119	23	Readout origin
EMEC	A	10L	18	B1	9	63	110	Readout origin
EMEC	A	13L	24	M3	13	94	55	Readout origin
EMEC	C	6R	2	F0	2	84	12	Calibration origin
EMEC	C	3R	7	B0	8	118	95	Readout origin
EMEC	C	3L	7	M3	13	78	55	Readout origin
EMEC	C	3L	7	M3	13	110	119	Readout origin
EMEC	C	2R	9	F4	6	14	50	Calibration origin
EMEC	C	2R	9	F4	6	16	48	Readout origin, leaking
EMEC	C	1R	11	B1	9	120	122	Readout origin
EMEC	C	1R	11	M3	13	4	50	Readout origin

Table 8: List of the dead channels in the EMEC analyzed with crosstalk.

Det.	Side	Crate	FT	FEB	Slot	Channel	Calibration line	Comments
EMB	A	I02	1	F6	8	120	0	Calibration origin
EMB	A	I04	5	F2	4	52	32	Calibration origin
EMB	A	I04	5	F2	4	53	33	Calibration origin
EMB	A	I04	5	F2	4	54	34	Calibration origin
EMB	A	I04	5	F2	4	55	35	Calibration origin
EMB	A	I04	6	M1	12	127	58	Calibration origin
EMB	A	I05	8	F6	8	117	97	Readout origin
EMB	A	I05	8	F6	8	125	97	Readout origin
EMB	A	I06	9	F1	3	10	18	Readout origin
EMB	A	I06	9	F3	5	25	49	Readout origin
EMB	A	I06	9	F3	5	33	49	Readout origin
EMB	A	I06	9	F4	6	40	64	Calibration origin
EMB	A	I08	14	B0	9	65	13	Readout origin
EMB	A	I11	20	F6	8	82	98	Readout origin
EMB	A	I11	20	M2	13	92	75	Calibration origin
EMB	A	I12	22	M3	14	44	103	Calibration origin
EMB	A	I12	22	M3	14	45	102	Calibration origin
EMB	A	I12	22	M3	14	47	102	Calibration origin
EMB	A	I12	22	M3	14	62	107	Calibration origin
EMB	A	I12	22	M3	14	63	106	Calibration origin
EMB	A	I15	28	F2	4	117	35	Calibration origin
EMB	A	I15	28	B1	10	62	114	Calibration origin
EMB	A	I16	29	B1	10	57	0	Calibration origin
EMB	A	I00	31	F3	5	48	0	Calibration origin
EMB	A	I00	31	F3	5	71	0	Calibration origin
EMB	A	I00	31	F4	6	84	0	Calibration origin
EMB	C	H09	0	F4	6	91	67	Readout origin, leaking
EMB	C	H08	1	B1	10	113	113	Calibration origin
EMB	C	H06	5	F4	6	77	0	Calibration origin
EMB	C	H04	9	F4	6	32	0	Calibration origin
EMB	C	H04	10	M1	12	8	0	Calibration origin
EMB	C	H11	27	M2	13	95	74	Calibration origin
EMB	C	H10	29	B1	10	102	110	Readout origin
EMB	C	H10	30	F6	8	7	0	Readout origin

Table 9: List of the distorted channels in the barrel analyzed with crosstalk.

Det.	Side	Crate	FT	FEB	Slot	Channel	Calibration line	Comments
EMEC	A	1R	0	F1	3	96	65	Readout origin
EMEC	A	1R	0	F5	7	93	97	Readout origin
EMEC	A	2R	2	F1	5	68	40	Calibration origin
EMEC	A	3R	4	M0	10	2	4	Calibration origin
EMEC	A	3L	5	F2	4	32	16	Readout origin
EMEC	A	3L	5	F2	4	37	17	Calibration origin
EMEC	A	3L	5	F2	4	49	17	Calibration origin
EMEC	A	3L	5	F3	5	119	83	Readout origin, leaking
EMEC	A	3L	5	M3	13	60	115	Calibration origin
EMEC	A	5R	7	F5	7	70	98	Calibration origin
EMEC	A	6R	9	M0	3	11	2	Calibration origin
EMEC	A	6R	9	F1	5	0	32	Readout origin, leaking
EMEC	A	7L	12	M0	10	32	68	Calibration origin
EMEC	A	8L	14	F5	7	48	32	Calibration origin
EMEC	A	8L	14	F5	7	52	32	Calibration origin
EMEC	A	8L	14	F5	7	56	32	Calibration origin
EMEC	A	8L	14	F5	7	60	32	Calibration origin
EMEC	A	9R	15	F5	12	0	64	Calibration origin
EMEC	A	10L	18	F4	6	42	34	Readout origin, leaking
EMEC	A	10L	18	F5	7	43	35	Readout origin, leaking
EMEC	A	11R	19	F5	7	64	96	Readout origin, leaking
EMEC	A	11R	19	F5	7	84	96	Readout origin
EMEC	A	11R	19	F5	7	85	97	Readout origin
EMEC	A	11R	19	F5	7	86	98	Readout origin
EMEC	A	11R	19	F5	7	87	99	Readout origin
EMEC	A	11R	19	F5	7	88	96	Readout origin
EMEC	A	11R	19	F5	7	89	97	Readout origin
EMEC	A	11R	19	F5	7	90	98	Readout origin
EMEC	A	11R	19	F5	7	91	99	Readout origin
EMEC	A	12R	21	B1	13	71	96	Calibration origin

Table 10: List of distorted channels in the EMEC-A analyzed with crosstalk.

Det.	Side	Crate	FT	FEB	Slot	Channel	Calibration line	Comments
EMEC	C	7R	0	F1	3	24	0	Readout origin, leaking
EMEC	C	7L	1	F1	3	121	65	Readout origin, leaking
EMEC	C	7L	1	M1	11	42	85	Readout origin, leaking
EMEC	C	6R	2	M1	4	27	2	Calibration origin
EMEC	C	6R	2	M1	4	86	16	Calibration origin
EMEC	C	6R	2	M1	4	91	14	Calibration origin
EMEC	C	6R	2	F3	7	0	32	Readout origin
EMEC	C	6R	2	F5	12	94	90	Readout origin
EMEC	C	6R	2	F5	12	95	91	Readout origin, leaking
EMEC	C	5L	5	F5	7	39	35	Readout origin
EMEC	C	5L	5	M0	10	119	75	Calibration origin
EMEC	C	2R	9	F2	6	2	50	Calibration origin
EMEC	C	2R	9	F5	12	29	89	Calibration origin
EMEC	C	2R	9	F5	12	71	67	Readout origin, leaking
EMEC	C	2R	9	M4	14	25	68	Calibration origin
EMEC	C	12R	15	M4	14	15	70	Calibration origin
EMEC	C	12R	15	M4	14	92	87	Calibration origin
EMEC	C	12R	15	M4	14	108	95	Calibration origin
EMEC	C	11R	17	B1	9	71	56	Readout origin
EMEC	C	11L	18	F5	7	127	99	Readout origin, leaking
EMEC	C	10R	19	F0	2	126	66	Calibration origin
EMEC	C	9R	21	F5	12	93	89	Calibration origin
EMEC	C	8R	23	F0	2	69	65	Readout origin

Table 11: List of the distorted channels in the EMEC-C analyzed with crosstalk.

Detector	Side	Crate	Feedthrough	FEB	slot	Swapped channels
EMB	A	I04	6	F0	2	112 \rightarrow 119 and 120 \rightarrow 127
EMB	A	I10	17	F1	3	112 \rightarrow 119 and 120 \rightarrow 127
EMB	A	I12	22	F5	7	32 \rightarrow 39 and 40 \rightarrow 47
EMB	C	H09	0	F6	8	32 \rightarrow 39 and 40 \rightarrow 47
EMB	C	H06	5	F4	6	ϕ -regions swapping
EMB	C	H10	29	F3	5	ϕ -regions swapping
EMB	C	H10	29	F5	7	ϕ -regions swapping

Table 12: List of found channels swapping. The ϕ -regions swapping correspond to the swap of the channels 0 \rightarrow 63 and 64 \rightarrow 127. The other inversions are motherboard connectors swapping.

Detector	Side	Crate	Feedthrough	Channels	Comments
EMB	A	I02	2	F5 8 and 9	Short in signal layer
EMB	A	I06	10	F0 80 and 81	Short in HV layer
EMB	A	I12	22	B1 107 and M3 55	Short in HV layer
EMB	C	H04	9	F0 59 and 60	Short in signal layer

Table 13: List of seen shorts in the barrel.